
Scalable and Adaptive Graph Neural Networks with Self-Label-Enhanced training

Chuxiong Sun

Beijing Research Institute

China Telecom Corporation Limited

Beijing, China

chuxiongsun@gmail.com

Guoshi Wu

School of Software Engineering

Beijing University of Posts and Telecommunications

Beijing, China

buptsse.gwu@gmail.com

Abstract

It is hard to directly implement Graph Neural Networks (GNNs) on large scaled graphs. Besides of existed neighbor sampling techniques, scalable methods decoupling graph convolutions and other learnable transformations into preprocessing and post classifier allow normal minibatch training. By replacing redundant concatenation operation with attention mechanism in SIGN, we propose Scalable and Adaptive Graph Neural Networks (SAGN). SAGN can adaptively gather neighborhood information among different hops. To further improve scalable models on semi-supervised learning tasks, we propose Self-Label-Enhance (SLE) framework combining self-training approach and label propagation in depth. We add base model with a scalable node label module. Then we iteratively train models and enhance train set in several stages. To generate input of node label module, we directly apply label propagation based on one-hot encoded label vectors without inner random masking. We find out that empirically the label leakage has been effectively alleviated after graph convolutions. The hard pseudo labels in enhanced train set participate in label propagation with true labels. Experiments on both inductive and transductive datasets demonstrate that, compared with other sampling-based and sampling-free methods, SAGN achieves better or comparable results and SLE can further improve performance.

1 Introduction

Graph neural networks (GNNs) have state-of-the-art performances on graph related tasks [1–12]. But many GNNs [1, 13–15] have problems of scalability and generalization with partial labels. In industrial scenarios, it is hard to scale common GNN models on huge graphs. From another aspect, in semi-supervised learning tasks, GNNs can be further improved by self-training approaches and label propagation [16–21]. In this paper, we focus on improving GNNs on large-scaled graphs with semi-supervised learning tasks.

GNNs on huge graphs For large scaled graphs, it is hard to apply GNNs with minibatch training. Because the receptive field of sampled nodes is variable and its size grows exponentially with layers. The neighbor sampling methods [22–29] have been proven to be effective to scale GNNs to large graphs by sampling a small part of neighboring nodes. As another way, we can decouple global smoothing operations and learnable transformations into preprocessing/postprocessing and a scalable classifier [30, 31]. Then we can directly apply mini-batch training since the input of the classifier is Euclidean. We conclude such methods as scalable or sampling-free GNNs.

Based on scalable methods, we propose **S**calable and **A**daptive **G**raph neural **N**etworks (**SAGN**). SAGN incorporates learnable attention weights between multiple hops [32], which improves the performance and interpretability.

GNNs on semi-supervised learning tasks The self-training approach [33–36] can improve model performance on semi-supervised learning tasks, including graph related ones [16–18]. From another aspect, the label propagation [19, 20, 37–39] can bring valuable information. The inner random masking within train set [19, 40] is required to prevent the label leakage which leads to a trivial solution. In scalable GNNs, if this masking operation is done for every epoch then the associated label propagation will cost much runtime. However, we find that empirically the label leakage is already effectively reduced after graph convolutions for many datasets. Then we can directly propagate one-hot encoded label embedding in the graph. Moreover, the pseudo labels can naturally participate in label propagation.

Thus we propose the **S**elf-**L**abel-**E**nhaned (**SLE**) approach for semi-supervised graph learning tasks, which effectively combines self-training and label propagation. Firstly, to incorporate label information, we propose scalable node label module compatible with any scalable base model. Secondly, following self-training approaches, we split the training process into stages with enhancing train set. Thirdly, the hard pseudo labels in self-training participate in label propagation in the preprocessing of node label module.

Contributions In conclusion, we propose a scalable GNN (SAGN) and a training framework (SLE) for large scaled graphs with semi-supervised learning tasks. Our main contributions are: 1. We incorporate learnable attention mechanism into scalable GNNs to obtain better expressiveness and interpretability with considerable complexity. 2. We firstly propose that empirically graph convolutions can effectively alleviate the label leakage without inner random masking, which makes it feasible to incorporate label information into scalable GNNs. 3. We firstly propose a general training framework effectively combining self-training and label propagation to boost scalable methods on large scaled graph data.

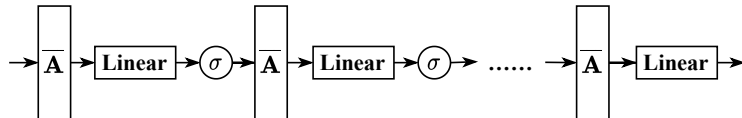
Experiments We conduct experiments on both inductive and transductive datasets including the largest public node classification dataset. SAGN scales well to web-scale data. And SAGN achieves better results compared with other sampling-based and sampling-free baselines on most datasets. SLE significantly boosts performance of SAGN with relative improvements up to 8.4%.

2 Background and related works

Graph neural networks The spectral GNNs [1, 41, 42] usually require complex eigendecomposition of laplacian matrix. ChebyNet proposes a simplified approximation method [42–44]. GCN [1] further limits the approximation order and adds self-loops. The spatial GNNs, including GCN, GAT [14] and GIN [15], perform direct neighborhood aggregations in graphs.

Sampling-based Methods The neighbor sampling methods can be classified into node-wise, layer-wise and graph-wise methods. Node-wise methods [22, 23, 26] sample smaller number of neighbors for each node. Layer-wise methods [24, 25] avoid the redundant sampling of node-wise methods. Graph-wise methods [28, 29] partition graph and limit convolutions in smaller subgraphs.

Scalable GNNs As shown in Figure 1, common GNNs alternately stack graph convolutions, linear layers and non-linear activation functions to generate non-linear hierarchies. As shown in Figures 2 and 3, models [30, 31] are decoupled into preprocessing and scalable classifiers. The classifiers have Euclidean input and are much easier to apply minibatch training.



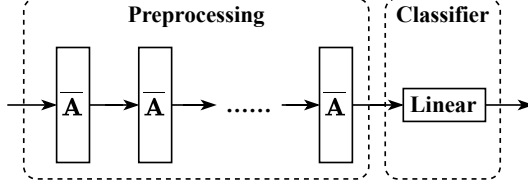


Figure 2: Architecture of SGC.

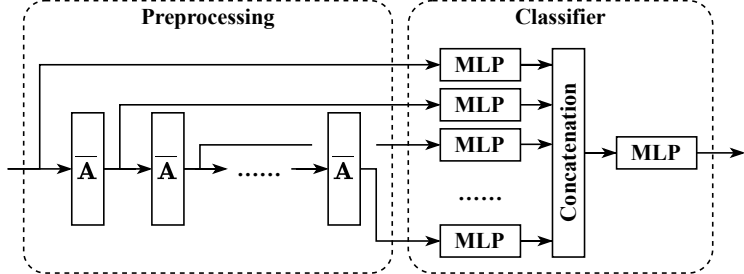


Figure 3: Architecture of SIGN.

As shown in Figure 2, SGC [30] uses linear layer as the post classifier. SGC firstly points out that empirically the removal of intermediate non-linear activations does not significantly affect the model performance. SGC achieves comparable performances in small datasets with much faster training and inference. However, the single linear layer limits expressiveness and multi-hop information is lost.

As shown in Figure 3, SIGN [31] uses more complex multi-layer perceptrons (MLP) and inception-like module [45]. Firstly, each aggregation is passed through its associated MLP encoder. Secondly, SIGN concatenates encoded representations and forwards into a post MLP classifier to obtain final results. The multi-hop MLP encoders before concatenation can somehow approximate non-linear hierarchies of common GNNs. The post MLP encoder has greater expressiveness than linear layer. With suitable settings, SIGN can be viewed as ChebyNet, GCN and SGC [31]. However, the concatenation operation is naive and brings extra memory cost.

Self-training approach on graphs We can enhance the train set with more "pseudo-labeled" nodes to improve GNNs via self-training approaches [16–18]. In the traditional self-training process, we firstly train a model based on train set. Then we generate pseudo labels to enhance train set. With enhanced train set we can train the next model. By repeating these steps for several times we obtain the final model. Li et al. [16] firstly propose co-training and self-training approaches on GNNs. Self-Enhanced GNN [18] incorporates topology update before enhancing the train set. It denoises the node relations by adding intra-class edges and removing inter-class edges based on predicted labels. The model knowledge is incorporated into both aligned structure and pseudo labels to train a stronger model. However, low-quality predictions can remove valuable edges and add redundant edges. Sun et al. [17] propose Multi-Stage Training Framework (M3S) combined with DeepCluster approach [46]. In details, it performs DeepCluster on the trained node representations and aligns cluster labels with true labels to obtain pseudo labels. M3S expects that the nodes in the same cluster are more likely to share the same label.

Label propagation Besides of enhancing train set, we can also perform label propagation to improve performance. A simple method is to concatenate node features and one-hot encoded label embeddings [40]. UniMP [19] adds node feature matrix with transformed label embedding matrix. GCN-LPA [20] uses label propagation prior in computing edge weights. Huang et al. [21] find an interesting and efficient way named as C&S. C&S firstly propagates residuals (or corrections) of simple base model into unlabeled nodes. Secondly it performs label smoothing [47]. Since C&S is non-parameterized postprocessing, it can be combined with any base model including MLP, GCN, etc. For non GNN like methods, it requires extra preprocessing including spectral and diffusion [48] calculation.

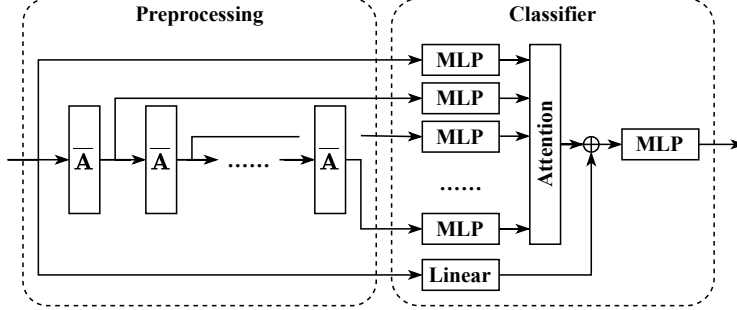


Figure 4: Architecture of SAGN.

3 Proposed methods

3.1 SAGN

The overall architecture of SAGN is shown in Figure 4. We will successively present the preprocessing, multi-hop encoders, attention mechanism and post encoder of SAGN. Let \mathcal{G} represent a graph, \mathcal{N} represent its node set, \mathcal{E} represent its edge set, X represent its node feature matrix, C represent the number of classes, \mathbf{A} represent its adjacency matrix, N represent its node number and E represent its edge number.

Preprocessing Suppose that we want to gather neighborhood node features within K_f -hop convolutions. We set $\bar{X}^{(0)} = X$. The k -hop smoothed node feature matrix $\bar{X}^{(k)}$ ($k > 0$) is computed as below:

$$\bar{X}^{(k)} = \bar{A} \bar{X}^{(k-1)}, \quad (1)$$

where \bar{A} is the non-parametric transition matrix [48] which can be row-stochastic random walk matrix, symmetrically normalized adjacency matrix, etc.

Multi-hop encoders SAGN uses multi-hop node features as input. To obtain the k -hop representation $H^{(k)}$, we apply an encoder $\zeta^{(k)}$ as below:

$$H^{(k)} = \zeta^{(k)}(\bar{X}^{(k)}). \quad (2)$$

Attention mechanism Then we sum different encoded representations with diagonal attention matrices [14, 32]. With adding a residual term we obtain the integrated representation H_{att} as below:

$$H_{att} = \sum_{k=0}^{K_f} \Theta^{(k)} H^{(k)} + X W_r, \quad (3)$$

where $\Theta^{(k)}$ is the k -th diagonal attention matrix and W_r is the residual linear matrix. The i -th entry $\theta_i^{(k)}$ of $\Theta^{(k)}$ is calculated as below:

$$\theta_i^{(k)} = \text{softmax}(\text{LeakyReLU}([H_i^{(0)} || H_i^{(k)}] \cdot a)), \quad (4)$$

where a is the attention vector. The concatenation operation in SIGN is equal to summing with uniform weights and brings redundant memory cost. The proof can be found in Appendix.

Post encoder We further feed the integrated representation into the post encoder ξ to generate output representation H_f of SAGN:

$$H_f = \xi(H_{att}). \quad (5)$$

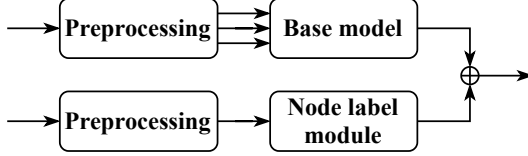


Figure 5: Architecture of model in SLE.

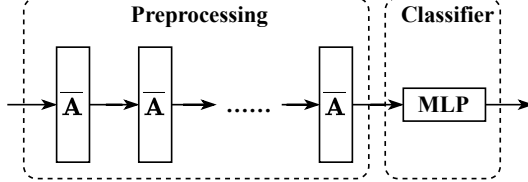


Figure 6: Architecture of node label module.

3.2 SLE

We propose Self-Label-Enhance (SLE) training framework to combine self-training and label propagation. We will present this framework from aspects of model architecture, training process and loss function. The enhanced train set and its complementary set at the s -stage are respectively represented with \mathcal{L}_s and \mathcal{U}_s . Y represents the raw one-hot encoded label embedding. \hat{Y}_s and \tilde{Y}_s respectively represent soft and hard output labels of the s -th model. Note that Y is zero vector for nodes out of raw train set.

Model architecture For scalable base models including MLP, SGC, SIGN and SAGN, we add with node label module. In details, as shown in Figure 5, the node feature information and label information are respectively passed through base model and node label module. The node label module can be common models such as MLP.

For each stage s , firstly the initial 0-hop label embedding is calculated. We set the initial label embedding at the first stage $\bar{Y}_0^{(0)} = Y$. From the second stage, the initial label embedding $\bar{Y}_s^{(0)}$ is calculated with ground truth labels and hard pseudo labels:

$$\bar{Y}_{s,i}^{(0)} = \begin{cases} Y_i, & i \in \mathcal{L}_0 \\ \tilde{Y}_{s-1,i}, & i \in \mathcal{L}_s \setminus \mathcal{L}_0 \\ [0, 0, \dots, 0], & i \in \mathcal{U}_s \end{cases}, \quad (6)$$

where i represents the node i .

Then label propagation with maximum hop of K_l is computed as below:

$$\bar{Y}_s^{(k)} = \bar{A} \bar{Y}_s^{(k-1)}, \quad (7)$$

where $\bar{Y}_s^{(k)}$ is the k -hop ($k > 0$) node label embedding matrix.

To reduce the label leakage, only the last label embedding $\bar{Y}_s^{(K_l)}$ is used. We apply encoder ϕ_s to this embedding:

$$(H_l)_s = \phi_s(\bar{Y}_s^{(K_l)}). \quad (8)$$

With using SAGN as base model for example, we sum outputs from base model (with adding subscript s) and node label module to obtain the final representation matrix H_s as below:

$$H_s = \xi_s \left(\sum_{k=0}^{K_f} \Theta_s^{(k)} \zeta_s^{(k)} (\bar{A}^k X) + X(W_r)_s \right) + \phi_s(\bar{A}^{K_l} \bar{Y}_s^{(0)}). \quad (9)$$

Table 1: Summary of datasets. For classes, there are single (s) label classification task and multiple (m) label classification task.

Dataset	Nodes	Edges	Classes	Train/Val/Test	Setting
Reddit	232,965	11,606,919	41(s)	66% / 10% / 24%	Inductive
Yelp	716,847	6,977,410	100(m)	75% / 10% / 15%	Inductive
Flickr	89,250	899,756	7(s)	50% / 25% / 25%	Inductive
PPI	14,755	225,270	121(m)	66% / 12% / 22%	Inductive
ogbn-products	2,449,029	61,859,140	47(s)	10% / 2% / 88%	Transductive
ogbn-papers100M	111,059,956	1,615,685,872	172(s)	78% / 8% / 14%	Transductive
ogbn-mag	1,939,743	21,111,007	349(s)	85% / 9% / 6%	Transductive

Training process We split training process into stages. At the first stage, we train a model with raw train set. Starting from the second stage, we enhance train set with previous predicted probabilities and train a new model. After certain stages we obtain the final model.

To enhance train set, we firstly obtain the confident node set at the s -stage $\bar{\mathcal{L}}_s$ ($s > 0$) with a threshold a as below:

$$\bar{\mathcal{L}}_s = \{i, \max_c(\hat{Y}_{s-1,i,c}) \geq a\} \subset \mathcal{N}. \quad (10)$$

Then the enhanced train set at the s -stage \mathcal{L}_s is updated as below:

$$\mathcal{L}_s = \mathcal{L}_0 \cup \bar{\mathcal{L}}_s. \quad (11)$$

Loss function We do not use KD loss [49], since it conflicts with hard pseudo labels and empirically brings no improvements. The loss function of SLE at the s -stage is calculated as below:

$$L_s = \frac{1}{|\mathcal{L}_s|} \left(\sum_i \sum_c Y_{i,c} \log(\hat{Y}_{s,i,c}) + \sum_j \sum_c \tilde{Y}_{s-1,j,c} \log(\hat{Y}_{s,j,c}) \right), \quad (12)$$

where c represents the c -th class, $|\mathcal{L}_s|$ is the element number of \mathcal{L}_s , i satisfies $i \in \mathcal{L}_0$ and j satisfies $j \in \mathcal{L}_s \setminus \mathcal{L}_0$.

4 Experiments and analysis

Datasets We evaluate our proposed method on both inductive (Reddit, Flickr, PPI and Yelp) and transductive (ogbn-products, ogbn-papers100M and ogbn-mag) datasets. The detailed descriptions of datasets and experiments on heterogeneous ogbn-mag [50] are reported in Appendix. The statistics of these datasets are listed in Table 1.

Inductive settings In the inductive setting [22, 29, 51], the nodes out of train set are forbidden to participate in model training but allowed in inference. With SLE, from the second stage, we actually use node features out of raw train set when training. However, we do not rely on the prior that the nodes from different sets have inter-set edges in transductive setting. Moreover, we still restrict graph convolutions in raw train graph(s) for nodes belonging to raw train set when training with enhanced train set. It meets the actual condition when applying the model on unseen data.

Special notations In experimental results, s -SLE ($s > 0$) means that we train the model under SLE framework after s stages. SE refers to SLE framework without node label module, which is equal to self-training [16]. 0-SLE means that we train base model with node label module using raw train set. The notation 0-SE is negligible since there are no modifications.

Baselines and hardware configuration We select vanilla (R)GCN [1, 52], UniMP [19], sampling-based GNNs [22–29] and sampling-free methods [21, 30, 31, 53–55] as baselines. For baselines we use metrics from official reports and OGB leaderboard [50]. For our proposed methods, we conduct experiments with pytorch and DGL [56] on a China Telecom Cloud p2v.16xlarge.8 instance, with

Table 2: Results on inductive datasets. The means and standard deviations of micro-F1 score over 10 runs are reported. The best results are highlighted in **bold** fonts.

Method	Reddit	Flickr	PPI	Yelp
GCN [1]	93.3 \pm 0.0%	49.2 \pm 0.3%	51.5 \pm 0.6%	37.8 \pm 0.1%
FastGCN [25]	92.4 \pm 0.1%	50.4 \pm 0.1%	51.3 \pm 3.2%	26.5 \pm 5.3%
Stochastic-GCN [26]	96.4 \pm 0.1%	48.2 \pm 0.3%	96.3 \pm 1.0%	64.0 \pm 0.2%
AS-GCN [24]	95.8 \pm 0.1%	50.4 \pm 0.2%	68.7 \pm 1.2%	—
GraphSAGE [22]	95.3 \pm 0.1%	50.1 \pm 1.3%	63.7 \pm 0.6%	63.4 \pm 0.6%
ClusterGCN [28]	95.4 \pm 0.1%	48.1 \pm 0.5%	87.5 \pm 0.4%	60.9 \pm 0.5%
GraphSaint [29]	96.6 \pm 0.1%	51.1 \pm 0.1%	98.1\pm0.4%	65.3\pm0.3%
SGC [30]	94.9 \pm 0.0%	50.2 \pm 0.1%	89.2 \pm 1.5%	35.8 \pm 0.6%
SIGN [31]	96.8 \pm 0.0%	51.4 \pm 0.1%	97.0 \pm 0.3%	63.1 \pm 0.3%
SAGN	96.9 \pm 0.0%	51.4 \pm 1.2%	97.9 \pm 0.1%	65.3\pm0.1%
SAGN+1-SLE	97.1\pm0.0%	54.3 \pm 0.5%	98.0 \pm 0.1%	65.3\pm0.1%
SAGN+2-SLE	97.1\pm0.0%	54.6\pm0.4%	98.0 \pm 0.1%	65.3\pm0.1%

512G memory, 8 NVIDIA V100 GPUs, 64 vCPUs and a processor Intel(R) Xeon(R) Gold 6151 CPU @ 3.00GHz. We run for 10 times with the same random seed setting (from 0 to 9) for each experiment.

Inductive results For inductive datasets, at the first stage of SLE, we do not use node label module since the label propagation is restricted in train set when training in inductive setting. As shown in Table 2, SAGN outperforms baselines in most inductive datasets. For Reddit and Flickr, SAGN achieves close results to SIGN. For PPI and Yelp, SAGN outperforms SIGN by respectively 0.9% and 2.2%. It implies that the attention mechanism in SAGN is more effective for certain datasets in inductive setting. SAGN+1-SLE and SAGN+2-SLE both outperform their previous models. Although for most inductive datasets SLE brings few improvements, SLE improves performance significantly by 3.2% in Flickr. We can attribute to that in Flickr the label distribution follows smoothness assumption. For Yelp we remove node label module at all stages because empirically it brings no improvements. We hypothesise that in Yelp the smoothness assumption of labels is not well satisfied. Note that all hyperparameters are hand-tuned, while hyperparameters of SIGN are tuned using Bayesian optimization on inductive datasets.

Transductive results For ogbn-products, as shown in Table 3, SAGN outperforms SIGN by 0.68%. And SIGN outperforms MLP, Node2Vec, vanilla GCN and sampling-based methods by at least 0.25%. This implies that the inception-like module, MLP encoders and attention mechanism can bring stronger expressiveness. SAGN can be further improved by up to 1.30% with self-training. For methods using labels, SAGN+2-SLE achieves state-of-the-art results with 3.08% improvements based on SAGN. The performance also improves with stages increasing. Because SLE can tap potential of model with using label information. MLP+C&S also achieves close results, but it requires complex (though partial) decomposition of laplacian matrix. For the largest dataset ogbn-papers100M, as shown in Table 3, SAGN outperforms other methods without using label information by at least 1.07%. It can also be improved by 0.55% with self-training. With improvements of 1.25% based on SAGN, SAGN+2-SLE achieves state-of-the-art results. Full batch GCN, C&S and sampling-based methods have not been implemented for this dataset. UniMP is implemented with massive GPU memory. It is still outperformed by SAGN+SLE even at the first stage.

Complexity The complexity of SAGN is similar to SIGN [31]. Because they share the same preprocessing and similar architecture in post classifier. The complexity from attention mechanism is negligible compared to multi-hop encoders. We suppose that the layer numbers of multi-hop MLP encoders and post MLP encoder share the same order of magnitude L . We use d to represent hidden dimension and K to represent number of hops. The time complexity of SIGN and SAGN are shown in Table 4. SAGN has less complexity in post encoder. Finally, they share the same total time complexity $KLNd^2$ which is K times larger than MLP with the same layer number.

Table 3: Results on transductive datasets. The means and standard deviations of validation and test accuracies over 10 runs are reported. The best results are highlighted in **bold** fonts.

Method	ogbn-products		ogbn-papers100M	
	Validation	Test	Validation	Test
MLP	75.54 \pm 0.14%	61.06 \pm 0.08%	49.60 \pm 0.29%	47.24 \pm 0.31%
Node2Vec [50, 53]	90.32 \pm 0.06%	72.49 \pm 0.10%	58.07 \pm 0.28%	55.60 \pm 0.23%
GCN [1, 50]	92.00 \pm 0.03%	75.64 \pm 0.21%	—	—
GraphSAGE [22, 50]	92.24 \pm 0.07%	78.50 \pm 0.14%	—	—
NeighborSampling [22, 50]	91.70 \pm 0.09%	78.70 \pm 0.36%	—	—
ClusterGCN [28]	92.12 \pm 0.09%	78.97 \pm 0.33%	—	—
GraphSaint [29]	—	80.27 \pm 0.26%	—	—
SIGN [31, 56]	92.86 \pm 0.02%	80.52 \pm 0.13%	69.32 \pm 0.06%	65.68 \pm 0.06%
SAGN	93.09 \pm 0.04%	81.20 \pm 0.07%	70.34 \pm 0.99%	66.75 \pm 0.84%
SAGN+1-SE	92.54 \pm 0.04%	82.23 \pm 0.09%	70.79 \pm 0.12%	67.21 \pm 0.12%
SAGN+2-SE	92.33 \pm 0.03%	82.50 \pm 0.13%	70.89 \pm 0.12%	67.30 \pm 0.15%
UniMP	93.08 \pm 0.17%	82.56 \pm 0.31%	71.72 \pm 0.05%	67.36 \pm 0.10%
MLP+C&S	91.47 \pm 0.09%	84.18 \pm 0.07%	—	—
SAGN+0-SLE	93.27 \pm 0.04%	83.29 \pm 0.18%	71.06 \pm 0.08%	67.55 \pm 0.15%
SAGN+1-SLE	93.06 \pm 0.07%	84.18 \pm 0.14%	71.23 \pm 0.10%	67.77 \pm 0.15%
SAGN+2-SLE	92.87 \pm 0.03%	84.28\pm0.14%	71.31 \pm 0.10%	68.00\pm0.15%

Table 4: Time complexity analysis for scalable methods.

Method	Multi-hop encoders	Post encoder	Total
SIGN	$\mathcal{O}(KLNd^2)$	$\mathcal{O}((K + L)Nd^2)$	$\mathcal{O}(KLNd^2)$
SAGN	$\mathcal{O}(KLNd^2)$	$\mathcal{O}((K/d + L)Nd^2)$	$\mathcal{O}(KLNd^2)$
MLP	—	$\mathcal{O}(LNd^2)$	$\mathcal{O}(LNd^2)$

Runtime The runtime comparison between SIGN and sampling-based methods has been previously conducted [31]. In conclusion, SIGN has longer preprocessing runtime but faster training runtime and much faster inference runtime. We conduct runtime experiments on dataset ogbn-products with scalable baselines including MLP and SIGN. As shown in Table 5, SIGN and SAGN have very close runtimes in both training and inference process, as expected in complexity analysis. SAGN has 10% smaller memory cost and 36% less parameters compared with SIGN, which comes from the removal of concatenation operation. The node label module brings longer training time, a bit more memory cost and more parameters. However, the inference runtime seems stable for each base model, since there is no gradient computation in inference. In addition, we report SAGN+SLE on ogbn-papers100M with training runtime of 14.31 ± 1.22 seconds and inference runtime of 7.05 ± 0.68 seconds at each epoch.

Table 5: Runtime experiments on ogbn-products. The runtimes (seconds) with means and standard deviations, memory costs (Mb) and parameter numbers over 10 runs are reported. SIGN+SLE is not reported due to out-of-memory (OOM) error.

Method	Training	Inference	Memory	Parameters
MLP	0.67 \pm 0.04s	7.78 \pm 0.25s	10832Mb	669743
SIGN	1.27 \pm 0.10s	8.68 \pm 0.64s	15558Mb	3489847
SAGN	1.12 \pm 0.01s	8.43 \pm 0.22s	13948Mb	2233391
MLP+0-SLE	0.76 \pm 0.03s	7.85 \pm 0.30s	11958Mb	1181278
SAGN+0-SLE	1.47 \pm 0.01s	8.35 \pm 0.33s	14894Mb	2810462

Table 6: Ablation studies on ogbn-products. The means and standard deviations of validation and test accuracies over 10 runs are reported. SIGN+SLE is not reported due to OOM error. The best results in every stage are highlighted in **bold** fonts.

Method	0-stage	1-stage	2-stage
MLP+SE	$75.75 \pm 0.12\%$	$75.11 \pm 0.18\%$	$74.99 \pm 0.19\%$
SIGN+SE	$80.52 \pm 0.13\%$	$81.42 \pm 0.14\%$	$81.56 \pm 0.17\%$
SAGN*+SE	$80.25 \pm 0.09\%$	$81.35 \pm 0.08\%$	$81.47 \pm 0.11\%$
SAGN**+SE	$80.04 \pm 0.07\%$	$81.16 \pm 0.10\%$	$81.29 \pm 0.11\%$
SAGN+SE	$81.20 \pm 0.07\%$	$82.23 \pm 0.09\%$	$82.50 \pm 0.13\%$
SLE	$78.86 \pm 1.48\%$	$77.47 \pm 0.55\%$	$77.58 \pm 0.89\%$
MLP+SLE	$82.42 \pm 0.48\%$	$83.76 \pm 0.26\%$	$83.91 \pm 0.26\%$
SAGN*+SLE	$82.49 \pm 0.27\%$	$83.50 \pm 0.32\%$	$83.56 \pm 0.30\%$
SAGN**+SLE	$82.52 \pm 0.27\%$	$83.56 \pm 0.27\%$	$83.63 \pm 0.25\%$
SAGN+SLE	$83.29 \pm 0.18\%$	$84.18 \pm 0.14\%$	$84.28 \pm 0.14\%$

Ablation studies The ablation studies are conducted on ogbn-products. SAGN* and SAGN**, based on SAGN, respectively replace attention weights with uniform and exponentially decaying (with ratio of 0.5) weights. MLP uses the input of diffused feature matrix [48]. As shown in Table 6, both SAGN* and SAGN** are outperformed by SAGN with SE and SLE, which proves the effectiveness of attention mechanism. The results of SAGN* and SIGN are very close as expected. Each model with SLE outperforms the same base model with SE by at least 1.81%, which proves the effectiveness of node label module in SLE. Interestingly, MLP+SLE obtains better results than SAGN*+SLE and SAGN**+SLE. But MLP has worse results and cannot be improved with self-training. On the other hand, single node label module (SLE in Table 6) cannot either be improved with self-training. The combination of them brings instant improvement of at least 3.56%. Moreover, the combined model can be further improved by up to 1.49% with enhanced train set. We hypothesise that MLP captures less overlapping information with node label module than other base models. These results highlight the effectiveness of combination of base model and node label module, which brings both instant and potential improvements.

5 Conclusion

We propose sampling-free SAGN and general framework SLE for semi-supervised graph learning on large scaled data. With similar complexity and runtime to SIGN, SAGN achieves better expressiveness. SLE can further boost any base models including MLP, SIGN and SAGN. SAGN+SLE outperforms both sampling-based and sampling-free baselines on most datasets. Our proposed methods are easy to implement and extend on huge graphs with competitive performance.

Simplicity and expressiveness Scalable methods actually make a tradeoff between simplicity and expressiveness [31]. The predefined and precomputed graph convolutions may lose some initial information. To ensure considerable performance, it is intuitive to design complex post classifier with graph structure-aware components. For examples, SIGN using MLP and inception-like module outperforms SGC and SAGN using adaptive attention mechanism outperforms SIGN.

Limitations The transition matrix can play a key role in performance [31]. However, we focus on modifying post classifier to obtain better expressiveness with only two kinds of transition matrices in this paper. The multi-hop input requires large CPU memory cost proportional to hop number. SLE in some inductive datasets brings less improvements, since the graph architecture is different between training and inference. The enhanced train set with more nodes bring longer training runtime but faster converge speed. We can cutoff training at earlier steps.

References

- [1] Thomas N Kipf and Max Welling. Semi-supervised classification with graph convolutional networks. *arXiv preprint arXiv:1609.02907*, 2016.
- [2] Muhan Zhang and Yixin Chen. Link prediction based on graph neural networks. *arXiv preprint arXiv:1802.09691*, 2018.
- [3] Siyuan Qi, Wenguan Wang, Baoxiong Jia, Jianbing Shen, and Song-Chun Zhu. Learning human-object interactions by graph parsing neural networks. In *Proceedings of the European Conference on Computer Vision (ECCV)*, pages 401–417, 2018.
- [4] Federico Monti, Davide Boscaini, Jonathan Masci, Emanuele Rodola, Jan Svoboda, and Michael M Bronstein. Geometric deep learning on graphs and manifolds using mixture model cnns. In *Proceedings of the IEEE conference on computer vision and pattern recognition*, pages 5115–5124, 2017.
- [5] Nicholas Choma, Federico Monti, Lisa Gerhardt, Tomasz Palczewski, Zahra Ronaghi, Prabhat Prabhat, Wahid Bhimji, Michael M Bronstein, Spencer R Klein, and Joan Bruna. Graph neural networks for icecube signal classification. In *2018 17th IEEE International Conference on Machine Learning and Applications (ICMLA)*, pages 386–391. IEEE, 2018.
- [6] David Duvenaud, Dougal Maclaurin, Jorge Aguilera-Iparraguirre, Rafael Gómez-Bombarelli, Timothy Hirzel, Alán Aspuru-Guzik, and Ryan P Adams. Convolutional networks on graphs for learning molecular fingerprints. *arXiv preprint arXiv:1509.09292*, 2015.
- [7] Justin Gilmer, Samuel S Schoenholz, Patrick F Riley, Oriol Vinyals, and George E Dahl. Neural message passing for quantum chemistry. In *International Conference on Machine Learning*, pages 1263–1272. PMLR, 2017.
- [8] Sarah Parisot, Sofia Ira Ktena, Enzo Ferrante, Matthew Lee, Ricardo Guerrero, Ben Glocker, and Daniel Rueckert. Disease prediction using graph convolutional networks: application to autism spectrum disorder and alzheimer’s disease. *Medical image analysis*, 48:117–130, 2018.
- [9] Marinka Zitnik, Monica Agrawal, and Jure Leskovec. Modeling polypharmacy side effects with graph convolutional networks. *Bioinformatics*, 34(13):i457–i466, 2018.
- [10] Emanuele Rossi, Federico Monti, Michael Bronstein, and Pietro Liò. ncRNA classification with graph convolutional networks. *arXiv preprint arXiv:1905.06515*, 2019.
- [11] Federico Monti, Fabrizio Frasca, Davide Eynard, Damon Mannion, and Michael M Bronstein. Fake news detection on social media using geometric deep learning. *arXiv preprint arXiv:1902.06673*, 2019.
- [12] Pablo Gainza, Freyr Sverrisson, Federico Monti, Emanuele Rodola, D Boscaini, MM Bronstein, and BE Correia. Deciphering interaction fingerprints from protein molecular surfaces using geometric deep learning. *Nature Methods*, 17(2):184–192, 2020.
- [13] William L Hamilton, Rex Ying, and Jure Leskovec. Representation learning on graphs: Methods and applications. *arXiv preprint arXiv:1709.05584*, 2017.
- [14] Petar Veličković, Guillem Cucurull, Arantxa Casanova, Adriana Romero, Pietro Lio, and Yoshua Bengio. Graph attention networks. *arXiv preprint arXiv:1710.10903*, 2017.
- [15] Keyulu Xu, Weihua Hu, Jure Leskovec, and Stefanie Jegelka. How powerful are graph neural networks? *arXiv preprint arXiv:1810.00826*, 2018.
- [16] Qimai Li, Zhichao Han, and Xiao-Ming Wu. Deeper insights into graph convolutional networks for semi-supervised learning, 2018.
- [17] Ke Sun, Zhouchen Lin, and Zhanxing Zhu. Multi-stage self-supervised learning for graph convolutional networks on graphs with few labels, 2020.
- [18] Han Yang, Xiao Yan, Xinyan Dai, and James Cheng. Self-enhanced gnn: Improving graph neural networks using model outputs. *arXiv preprint arXiv:2002.07518*, 2020.
- [19] Yunsheng Shi, Zhengjie Huang, Shikun Feng, and Yu Sun. Masked label prediction: Unified message passing model for semi-supervised classification. *arXiv preprint arXiv:2009.03509*, 2020.
- [20] Hongwei Wang and Jure Leskovec. Unifying graph convolutional neural networks and label propagation. *arXiv preprint arXiv:2002.06755*, 2020.

- [21] Qian Huang, Horace He, Abhay Singh, Ser-Nam Lim, and Austin R Benson. Combining label propagation and simple models out-performs graph neural networks. *arXiv preprint arXiv:2010.13993*, 2020.
- [22] William L Hamilton, Rex Ying, and Jure Leskovec. Inductive representation learning on large graphs. *arXiv preprint arXiv:1706.02216*, 2017.
- [23] Rex Ying, Ruining He, Kaifeng Chen, Pong Eksombatchai, William L Hamilton, and Jure Leskovec. Graph convolutional neural networks for web-scale recommender systems. In *Proceedings of the 24th ACM SIGKDD International Conference on Knowledge Discovery & Data Mining*, pages 974–983, 2018.
- [24] Wenbing Huang, Tong Zhang, Yu Rong, and Junzhou Huang. Adaptive sampling towards fast graph representation learning. *arXiv preprint arXiv:1809.05343*, 2018.
- [25] Jie Chen, Tengfei Ma, and Cao Xiao. Fastgcn: fast learning with graph convolutional networks via importance sampling. *arXiv preprint arXiv:1801.10247*, 2018.
- [26] Jianfei Chen, Jun Zhu, and Le Song. Stochastic training of graph convolutional networks with variance reduction. *arXiv preprint arXiv:1710.10568*, 2017.
- [27] Difan Zou, Ziniu Hu, Yewen Wang, Song Jiang, Yizhou Sun, and Quanquan Gu. Layer-dependent importance sampling for training deep and large graph convolutional networks. *arXiv preprint arXiv:1911.07323*, 2019.
- [28] Wei-Lin Chiang, Xuanqing Liu, Si Si, Yang Li, Samy Bengio, and Cho-Jui Hsieh. Cluster-gcn: An efficient algorithm for training deep and large graph convolutional networks. In *Proceedings of the 25th ACM SIGKDD International Conference on Knowledge Discovery & Data Mining*, pages 257–266, 2019.
- [29] Hanqing Zeng, Hongkuan Zhou, Ajitesh Srivastava, Rajgopal Kannan, and Viktor Prasanna. Graphsaint: Graph sampling based inductive learning method. *arXiv preprint arXiv:1907.04931*, 2019.
- [30] Felix Wu, Amauri Souza, Tianyi Zhang, Christopher Fifty, Tao Yu, and Kilian Weinberger. Simplifying graph convolutional networks. In *International conference on machine learning*, pages 6861–6871. PMLR, 2019.
- [31] Emanuele Rossi, Fabrizio Frasca, Ben Chamberlain, Davide Eynard, Michael Bronstein, and Federico Monti. Sign: Scalable inception graph neural networks. *arXiv preprint arXiv:2004.11198*, 2020.
- [32] Chuxiong Sun and Guoshi Wu. Adaptive graph diffusion networks with hop-wise attention. *arXiv preprint arXiv:2012.15024*, 2020.
- [33] Jacob Kahn, Ann Lee, and Awni Hannun. Self-training for end-to-end speech recognition. In *ICASSP 2020-2020 IEEE International Conference on Acoustics, Speech and Signal Processing (ICASSP)*, pages 7084–7088. IEEE, 2020.
- [34] Junxian He, Jiatao Gu, Jiajun Shen, and Marc’Aurelio Ranzato. Revisiting self-training for neural sequence generation. *arXiv preprint arXiv:1909.13788*, 2019.
- [35] I Zeki Yalniz, Hervé Jégou, Kan Chen, Manohar Paluri, and Dhruv Mahajan. Billion-scale semi-supervised learning for image classification. *arXiv preprint arXiv:1905.00546*, 2019.
- [36] Qizhe Xie, Minh-Thang Luong, Eduard Hovy, and Quoc V Le. Self-training with noisy student improves imagenet classification. In *Proceedings of the IEEE/CVF Conference on Computer Vision and Pattern Recognition*, pages 10687–10698, 2020.
- [37] Zhu Xiaojin and Ghahramani Zoubin. Learning from labeled and unlabeled data with label propagation. *Tech. Rep., Technical Report CMU-CALD-02-107, Carnegie Mellon University*, 2002.
- [38] Fei Wang and Changshui Zhang. Label propagation through linear neighborhoods. *IEEE Transactions on Knowledge and Data Engineering*, 20(1):55–67, 2007.
- [39] Yasuhiro Fujiwara and Go Irie. Efficient label propagation. In *International Conference on Machine Learning*, pages 784–792. PMLR, 2014.
- [40] Yangkun Wang. Bag of tricks of semi-supervised classification with graph neural networks, 2021.

- [41] Joan Bruna, Wojciech Zaremba, Arthur Szlam, and Yann LeCun. Spectral networks and locally connected networks on graphs. *arXiv preprint arXiv:1312.6203*, 2013.
- [42] Michaël Defferrard, Xavier Bresson, and Pierre Vandergheynst. Convolutional neural networks on graphs with fast localized spectral filtering. *arXiv preprint arXiv:1606.09375*, 2016.
- [43] Ron Levie, Wei Huang, Lorenzo Bucci, Michael M Bronstein, and Gitta Kutyniok. Transferability of spectral graph convolutional neural networks. *arXiv preprint arXiv:1907.12972*, 2019.
- [44] Ron Levie, Federico Monti, Xavier Bresson, and Michael M Bronstein. Cayleynets: Graph convolutional neural networks with complex rational spectral filters. *IEEE Transactions on Signal Processing*, 67(1):97–109, 2018.
- [45] Christian Szegedy, Wei Liu, Yangqing Jia, Pierre Sermanet, Scott Reed, Dragomir Anguelov, Dumitru Erhan, Vincent Vanhoucke, and Andrew Rabinovich. Going deeper with convolutions. In *Proceedings of the IEEE conference on computer vision and pattern recognition*, pages 1–9, 2015.
- [46] Mathilde Caron, Piotr Bojanowski, Armand Joulin, and Matthijs Douze. Deep clustering for unsupervised learning of visual features. In *Proceedings of the European Conference on Computer Vision (ECCV)*, pages 132–149, 2018.
- [47] Johannes Klicpera, Aleksandar Bojchevski, and Stephan Günnemann. Predict then propagate: Graph neural networks meet personalized pagerank. *arXiv preprint arXiv:1810.05997*, 2018.
- [48] Johannes Klicpera, Stefan Weißenberger, and Stephan Günnemann. Diffusion improves graph learning. *arXiv preprint arXiv:1911.05485*, 2019.
- [49] Geoffrey Hinton, Oriol Vinyals, and Jeff Dean. Distilling the knowledge in a neural network. *arXiv preprint arXiv:1503.02531*, 2015.
- [50] Weihua Hu, Matthias Fey, Marinka Zitnik, Yuxiao Dong, Hongyu Ren, Bowen Liu, Michele Catasta, and Jure Leskovec. Open graph benchmark: Datasets for machine learning on graphs. *arXiv preprint arXiv:2005.00687*, 2020.
- [51] Marinka Zitnik and Jure Leskovec. Predicting multicellular function through multi-layer tissue networks. *Bioinformatics*, 33(14):i190–i198, 2017.
- [52] Michael Schlichtkrull, Thomas N. Kipf, Peter Bloem, Rianne van den Berg, Ivan Titov, and Max Welling. Modeling relational data with graph convolutional networks, 2017.
- [53] Aditya Grover and Jure Leskovec. node2vec: Scalable feature learning for networks. In *Proceedings of the 22nd ACM SIGKDD international conference on Knowledge discovery and data mining*, pages 855–864, 2016.
- [54] Lingfan Yu, Jiajun Shen, Jinyang Li, and Adam Lerer. Scalable graph neural networks for heterogeneous graphs. *arXiv preprint arXiv:2011.09679*, 2020.
- [55] Antoine Bordes, Nicolas Usunier, Alberto Garcia-Duran, Jason Weston, and Oksana Yakhnenko. Translating embeddings for modeling multi-relational data. In *Neural Information Processing Systems (NIPS)*, pages 1–9, 2013.
- [56] Minjie Wang, Da Zheng, Zihao Ye, Quan Gan, Mufei Li, Xiang Song, Jinjing Zhou, Chao Ma, Lingfan Yu, Yu Gai, Tianjun Xiao, Tong He, George Karypis, Jinyang Li, and Zheng Zhang. Deep graph library: A graph-centric, highly-performant package for graph neural networks. *arXiv preprint arXiv:1909.01315*, 2019.

A Appendix

A.1 Concatenation operation in SIGN

The concatenation operation with linear layer followed is equal to applying multiple linear layers and sum them up. This conclusion can be directly obtained by rules of matrix multiplication:

$$\left(\left| \left| \left| \begin{matrix} K \\ k=0 \end{matrix} \right| \right| \right) H^{(k)} W = \sum_{k=0}^K \left(H^{(k)} W^{(k)} \right). \quad (13)$$

$W^{(k)}$ is the k -th row slice of W with length of d :

$$W^{(k)} = W_{[kd:(k+1)d,:]}, \quad (14)$$

where d is the hidden dimension of $H^{(k)}$.

There are no tunable or learnable weights in the concatenation operation. It also increases the memory cost. Thus we explicitly sum representation matrices with learnable attention weights, which improves expressiveness and reduces memory cost with considerable additional complexity.

A.2 SLE Algorithm

The overall process of SLE framework is presented in Algorithm 1.

Algorithm 1: Self-Label-Enhanced training framework

Data: transition matrix \bar{A} , node feature X , node label Y , node set \mathcal{N} , class number C , set of labeled nodes (train set) \mathcal{L}_0 , set of unlabeled nodes \mathcal{U}_0 , maximum feature convolution hop K_f , maximum label propagation hop K_f , maximum stage S , threshold a

Result: final model $f_S + g_S$

- 1 precompute smoothed node features $\{\bar{X}^{(k)}\}$ ($0 \leq k \leq K_f$) using Eq. 1;
- 2 precompute label embedding $\bar{Y}_0^{(K_f)}$ using Eq. 6 and Eq. 7;
- 3 train the first model $f_0 + g_0$ with \mathcal{L}_0 and \mathcal{U}_0 ;
- 4 output soft labels \hat{Y}_0 and hard labels \tilde{Y}_0 ;
- 5 $s = 1$;
- 6 **while** $s \leq S$ **do**
- 7 $\bar{\mathcal{L}}_s = \{i, \max_c(\hat{Y}_{s-1,i,c}) \geq a\} \subset \mathcal{N}$;
- 8 $\mathcal{L}_s = \mathcal{L}_0 \cup \bar{\mathcal{L}}_s$, $\mathcal{U}_s = \mathcal{N} \setminus \mathcal{L}_s$;
- 9 precompute label embedding $\bar{Y}_s^{(K_f)}$ using Eq. 6 and Eq. 7;
- 10 train the s -th model $f_s + g_s$ using \mathcal{L}_s and \mathcal{U}_s ;
- 11 output soft labels \hat{Y}_s and hard labels \tilde{Y}_s ;
- 12 $s = s + 1$;
- 13 **end**

A.3 Hard pseudo labels

We aim to recover the label distribution of unlabeled nodes and propagate them with true labels in graphs. Unlike knowledge distillation, the recovered labels should be hard labels to align with the existed true labels. From another aspect, the hard pseudo labels without detailed probability distributions incorporates some moderate "noises" into teacher model's knowledge. With label propagation, these "noises" can also be propagated into other nodes. Then the model based on enhanced train set can more easily capture new knowledge. Meanwhile, to get high-quality pseudo labels and limit noises, we filter "confident" nodes. For examples, we can use a threshold-based or top-K filter to get confident nodes.

A.4 Dataset details

Reddit contains nodes representing posts in Reddit website with 300-dimensional GloVe Common-Crawl word vectors. An edge represents that two posts are commented by the same user. The node label represents its community. This is an inductive multi-class classification task. The time range of dataset is during the month of September, 2014. The first 20 days are used for training and the remaining days for testing.

In Flickr, the nodes represent pictures uploaded to the Flickr website with links representing they are from the same location, submitted to the same gallery, sharing common tags, etc. The node feature contains information of low-level feature. It is aimed to predict the tag of pictures, which is an inductive multi-class classification task. The train, validation and test nodes are randomly split into 0.5, 0.25 and 0.25.

PPI contains multiple subgraphs representing human tissues with proteins as nodes and protein interactions as edges. The positional gene sets, motif gene sets and immunological signatures are used as node features. We aim to predict protein roles, which is an inductive multi-label classification task. 20 graphs are used for training. Two graphs are used for testing with another two graphs for validation.

In Yelp, each node represents an active user and each edge represents a friendship relation. The node feature is generated from reviews of users using Word2Vec model. The task is to predict the types of business that the user has been to, which is an inductive multi-label classification task. The train, validation and test nodes are randomly split into 0.75, 0.10 and 0.15.

For ogbn-products, the graph represents an Amazon product co-purchasing network. Nodes represent products sold in Amazon. Edges represent that products are purchased together. Node features are 100-dimensional bag-of-words features from their descriptions. The task is to predict the category of a product, which is a transductive multi-class classification task. Instead of randomly splitting, The sales ranking (popularity) is used to split nodes into training, validation and test sets. Firstly the products are sorted according to their sales ranking. Secondly the top 8% is used for training, next top 2% is used for validation, and the rest is used for testing.

ogbn-papers100M is the largest node classification dataset. It contains up to 111 million nodes representing papers indexed by MAG and 1.6 billion edges representing citations. Each node has a 128-dimension feature vector by averaging the word embeddings of its title and abstract. The task is to predict the subject areas of the subset of papers published in arXiv (about 1.5 million). This is a transductive multi-class classification task. The training nodes with labels are all arXiv papers published until 2017, while the validation nodes are the arXiv papers published in 2018, and the models are tested on arXiv papers published since 2019.

ogbn-mag is a heterogeneous graph which is a subset from MAG. There are 736,389 "paper" nodes, 1,134,649 "author" nodes, 8,740 "institution" nodes and 59,965 "fields of study" nodes. For relations, an author "writes" a paper, an author is "affiliated with" an institution, a paper "cites" another paper and a paper "has a topic of" a field of study. Each paper node has a 128-dimension Word2Vec feature vector and other types of nodes do not have feature vectors. We aim to predict the venue of papers, which is a multi-class classification task. The way of splitting train, validation and test sets is the same as ogbn-papers100M.

A.5 Inductive setting

For most of datasets, all nodes are in the same graph. In PPI, the train, validation and test sets are totally separated without any inter-set edges. The propagation of both node feature and node label information is restricted in subgraphs. Although it is possible to apply SLE in such completely inductive setting, the distributions of label information vary between train set and other sets. Because we have full true labels in train sets but only parts of validation and test sets are filtered with pseudo labels. Even after smoothing, the label embeddings in train set and other sets can be very different. To further balance the distributions of label embedding in different sets, we also filter confident nodes in raw train set when generating initial label embedding. It means that, in raw train set, only nodes with high confidence have associated non-zero initial label embedding. In addition, the other nodes with zero initial label embedding still participate in model training.

A.6 Baseline selection

For Reddit, Flickr, PPI and Yelp, we select vanilla GCN, sampling-based GNNs and sampling-free GNNs as baselines. The neighbor sampling based GNNs include FastGCN, Stochastic-GCN, AS-GCN, GraphSAGE, ClusterGCN and GraphSaint. The sampling-free GNNs include SGC and SIGN.

For ogbn-products, Node2Vec, full-batch GCN, full-batch GraphSAGE, sampling-based GNNs and sampling-free methods are used as baselines. The sampling-based GNNs include NeighborSampling (SAGE), Cluster GCN, GraphSaint and UniMP. The scalable methods include MLP, SIGN and MLP + C&S. UniMP, MLP+C&S and SAGN+SLE incorporate label information.

For ogbn-papers100M, Node2Vec, UniMP and sampling-free methods are used as baselines. The naive methods include MLP and SIGN. UniMP and SAGN+SLE incorporate label information.

For ogbn-mag, MLP, vanilla GCN, GraphSAGE and SIGN are used as baselines in homogeneous setting and MetaPath2Vec, vanilla full-batch R-GCN, NeighborSampling (R-GCN), ClusterGCN, GraphSaint and NARS are used as baseline in heterogeneous setting.

A.7 Setup

For inductive setting, the train graph(s) are induced by removing inter edges between train set and evaluate sets. In the preprocessing of SAGN, the transition matrix is selected between symmetrically normalized adjacency matrix and row-stochastic random walk matrix. The former is used in GCN and works as a low-pass filter in the spectral domain. But recent researches show that, empirically, it is not always suitable to use this matrix. MLP encoders in SAGN share the same architecture with the same linear layer number (2, for example), batch normalizations and ReLU activation functions. The MLP encoder in node label module doubles the layer number of SAGN. The depth of node feature propagation K_f is tuned between 2 and 9. The depth of node label propagation K_l is tuned between 1 and 12. We filter confident nodes by threshold-based generator. For inductive setting, we do not use label embedding at the first stage. For datasets with multiclass tasks, we simply filter nodes whose maximum probability is greater than a certain threshold (between 0 and 1). For datasets with multilabel tasks, we filter nodes whose mean entropy in multiple labels is greater than a computed threshold between 0 and log2. Moreover, for multilabel tasks, we set the initial label embedding of nodes out of confident nodes to 0.5. Because in multilabel cases the most uncertain probability for each class is 0.5. Besides of standard weight decay and dropout techniques, we use attention dropout and input dropout. Specially, for ogbn-mag, we convert heterogeneous graph into homogeneous graph. However, nodes other than paper nodes have no raw node features. We follow two types of solutions: 1. Average their neighboring paper nodes' attributes to obtain equivalent attributes. 2. Use embedding vectors from pretrained TransE model. The latter also incorporates heterogeneous information in pretrained embeddings. The TransE embedding has been proven to be useful for heterogeneous graphs.

A.8 Experiments on ogbn-mag

Table 7 shows the results on ogbn-mag dataset with both homogeneous and heterogeneous settings. The means and standard deviations of validation and test accuracies are reported. For homogeneous settings, naive MLP achieves low test accuracy with mean 26.92%. Vanilla GCN improves the mean test accuracy to 30.43%. Sampling-based GraphSAGE improves GCN's result by 1%. Scalable SIGN effectively improves the mean test accuracy up to 40.46%. SAGN at the 1-stage slightly outperforms SIGN. But with enhanced train set SAGN brings the metric up to 42.75%. For heterogeneous setting, which more fits the heterogeneous graphs, MetaPath2Vec achieves 35.44% mean test accuracy. The vanilla full-batch R-GCN is outperformed by sampling-based methods except ClusterGCN. The cluster partitioning in ClusterGCN may in somehow break the initial data distribution. We use TransE embedding (with the dimension of 128) to incorporate heterogeneous information into SAGN. At the 0-stage, SAGN outperforms other naive and sampling-based methods. With stage increasing, SAGN improves the metric up to 50.29%. This score is higher than most of GNNs specially designed for heterogeneous graphs except NARS. NARS [54] uses TransE [55] embedding (with higher dimension of 256) and use subgraphs induced by sampled subrelations, which is also based on SIGN. By experiments on heterogeneous ogbn-mag dataset with directly adding TransE embedding, we prove that our proposed SAGN with SLE can achieve better or comparable results compared with other

Table 7: Results on ogbn-mag. Validation and test accuracies with means and standard deviations (%) are reported. The best results in homogeneous and heterogeneous settings are highlighted in **bold** fonts.

Method	Validation	Test
MLP	26.26 \pm 0.16%	26.92 \pm 0.26%
GCN	29.53 \pm 0.22%	30.43 \pm 0.25%
GraphSAGE	30.70 \pm 0.19%	31.53 \pm 0.15%
SIGN	40.68 \pm 0.10%	40.46 \pm 0.12%
SAGN+0-SLE	42.13 \pm 0.51%	40.51 \pm 0.83%
SAGN+1-SLE	43.85 \pm 0.49%	42.18 \pm 0.61%
SAGN+2-SLE	44.27 \pm 0.30%	42.75\pm0.38%
MetaPath2Vec	35.06 \pm 0.17%	35.44 \pm 0.36%
R-GCN	40.84 \pm 0.41%	39.77 \pm 0.46%
NeighborSampling	47.61 \pm 0.68%	46.78 \pm 0.67%
ClusterGCN	38.40 \pm 0.31%	37.32 \pm 0.37%
GraphSaint	48.37 \pm 0.26%	47.51 \pm 0.22%
NARS	53.72 \pm 0.09%	52.40\pm0.16%
SAGN+TransE+0-SLE	49.42 \pm 0.17%	47.95 \pm 0.25%
SAGN+TransE+1-SLE	51.23 \pm 0.16%	49.70 \pm 0.17%
SAGN+TransE+2-SLE	51.80 \pm 0.15%	50.29 \pm 0.16%

heterogeneous GNNs. We believe that incorporating heterogeneous model architecture into SAGN will bring better performance in heterogeneous graph learning tasks. But we leave this in the future discuss.

A.9 Runtime experiments

We also conduct extra runtime experiments of different stages on ogbn-products. As shown in Table 8, the training runtime increases with stage increasing. Because the enhanced train set contains much more nodes. However the model will converge faster.

Table 8: Runtimes experiments of different stages on ogbn-products. With additional nodes with pseudo labels, the training process costs more time. While the model converges in less epochs.

Method	Training	Inference	Memory
SAGN+0-SLE	1.47 \pm 0.01s	8.35 \pm 0.33s	14894Mb
SAGN+1-SLE	14.95 \pm 0.08s	8.42 \pm 0.39s	14894Mb
SAGN+2-SLE	17.01 \pm 0.18s	8.34 \pm 0.39s	14894Mb

A.10 Converge analysis

We record validation accuracies of different base models under SE and SLE at three stages on ogbn-products for every 10 epochs. As shown in Figure 7, with node label module, all models converge faster and have similar converge curves. As shown in Figures 8, 11, 9, 10 and 12, models converge faster with enhanced train set. Because the model at later stages can benefit from previous model’s output. To control training time without losing performance, we cutoff training models in earlier epochs at later stages in actual usage. A special case is that MLP cannot be improved by self-training without node label module. Although it still converges faster with enhanced train set. In contrast, MLP with node label module can be improved by self-training.

Overfitting from validation set With stages increasing, validation and test accuracies of SAGN are improved on ogbn-papers100M and ogbn-mag while validation accuracies become a bit lower on ogbn-products. We think that very low validation ratio (2%) in ogbn-products results in this

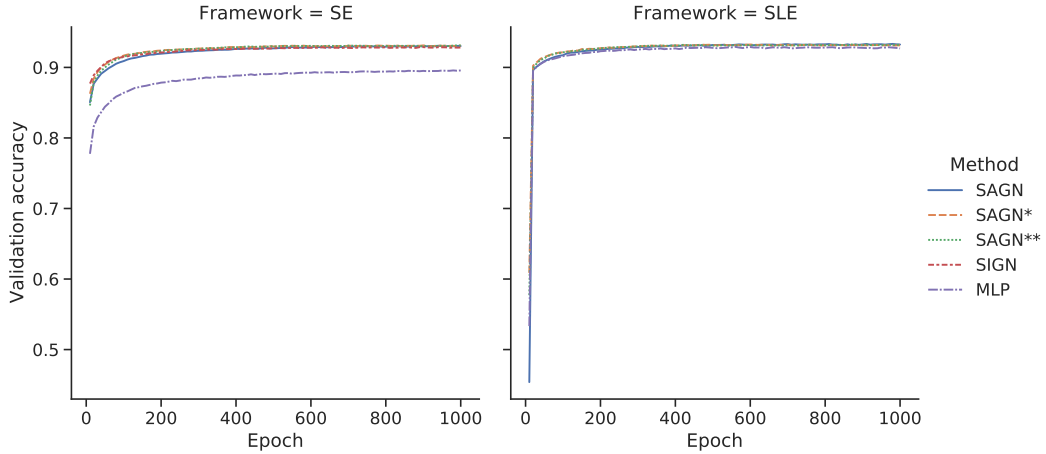


Figure 7: Converge statistics of different base models under SE and SLE at the first stage. The validation accuracy for every 10 epochs is reported.

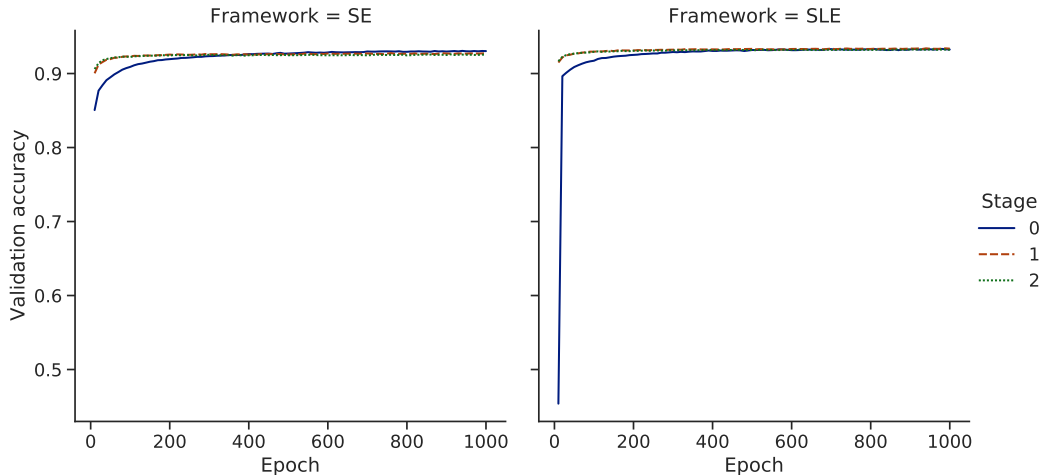


Figure 8: Converge statistics of SAGN under SE and SLE at 3 stages.

phenomenon. Because we select best model based on results of very few nodes from validation test. With enhanced train set containing nodes from both validation and test sets, the overfitting from best model selection on validation set is alleviated. Thus validation and test accuracies are more close and overall results are improved. In details, the validation accuracy is reduced and test accuracy is increased.

Table 9: Hyperparameter settings of SAGN+SLE for inductive datasets. At the first stage we do not use node label module.

Dataset	lr	hidden	norm	L	K_f	K_l	drop	$drop_a$	$drop_i$	batch_size	a	wd
Reddit	1e-4	512	row	2	2	4	0.7	0.0	0.0	1000	0.9	0
Flickr	1e-3	512	sym	2	2	2	0.7	0.0	0.0	256	0.5	3e-6
PPI	1e-3	1024	row	2	2	9	0.3	0.1	0.0	256	0.9	3e-6
Yelp	1e-4	256	row	2	2	6	0.05	0.0	0.0	200	0.9	5e-6

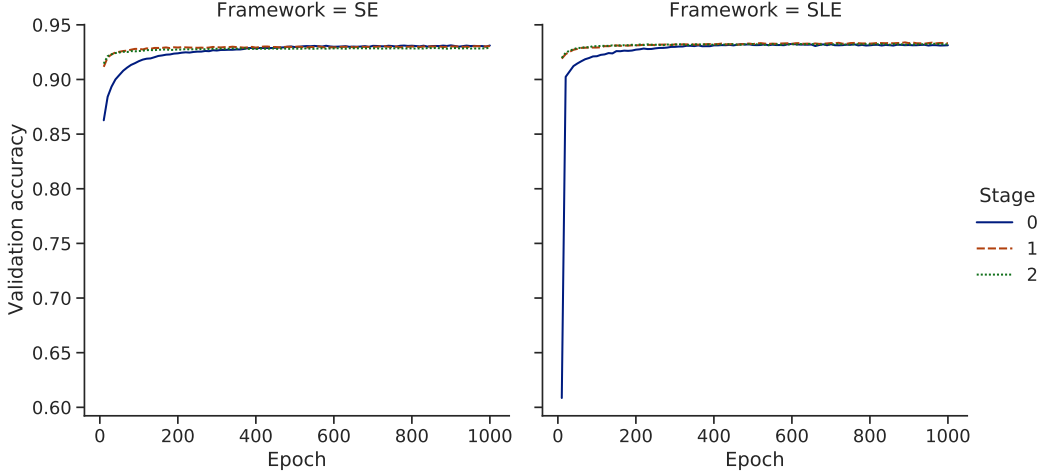


Figure 9: Converge statistics of SAGN* under SE and SLE at 3 stages.

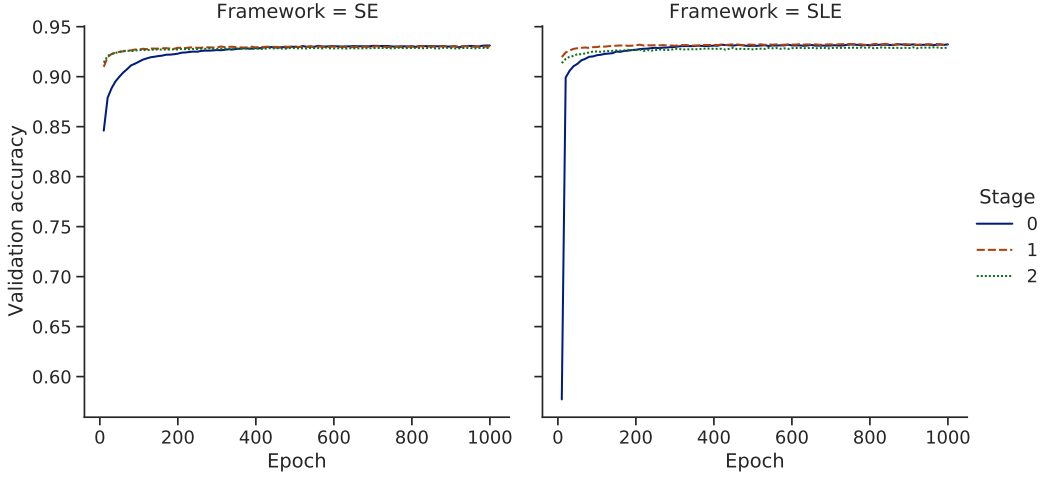


Figure 10: Converge statistics of SAGN** under SE and SLE at 3 stages.

A.11 Hyperparameter settings

For hyperparameters, we simply tune them empirically. Let lr represent learning rate, $hidden$ represent hidden dimension, $norm$ represent whether use symmetrically normalized adjacency matrix (sym) or row-stochastic random walk matrix (row), L represent layer number in MLP encoders, K_f represent hop number of node feature aggregations, K_l represent hop number of node label aggregations, $drop$ represent dropout ratio, $drop_a$ represent attention weights dropout ratio, $drop_i$ represent input dropout ratio, $batch_size$ represent batch size in training process, a represent threshold for filtering confident nodes and wd represent weight decay ratio. The hyperparameter settings for results in different datasets are shown in Table 9, Table 10, Table 11 and Table 12. Note that the settings of epoch numbers are omitted in tables. For Reddit, the epoch numbers are set to [500, 500, 500]. For Flickr, the epoch numbers are set to [50, 50, 50]. For PPI, the epoch numbers are set to [2000, 2000, 2000]. For Yelp, the epoch numbers are set to [100, 100, 100]. For ogbn-products, all methods use epoch numbers of [1000, 200, 200] except that MLP uses epoch numbers of [1000, 500, 500]. For ogbn-papers100M, the epoch numbers are set to [100, 50, 50]. For ogbn-mag, the epoch numbers are set to [200, 200, 200].

Ablation study SIGN, SAGN and its variants share the same MLP layer number of 2, hop number of 5 and hidden dimension of 512 except SAGN+SLE which uses a smaller hop number of 3.

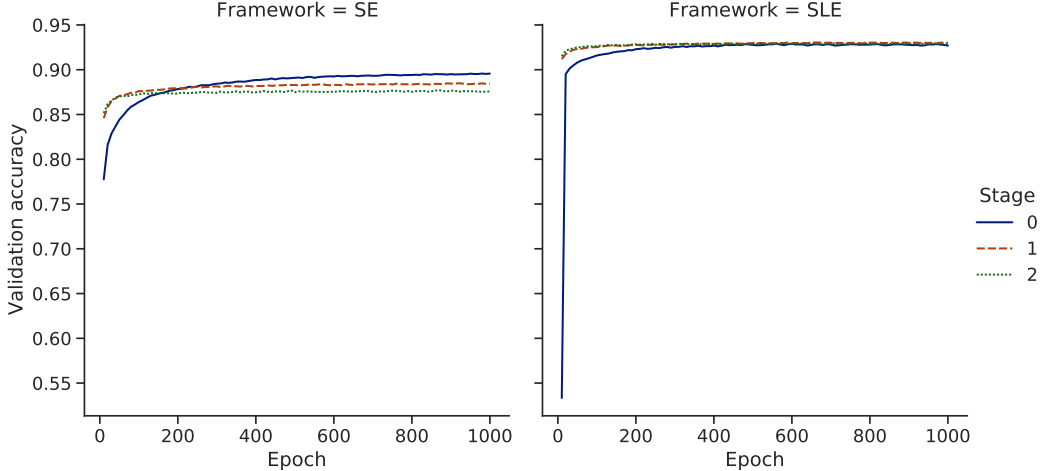


Figure 11: Converge statistics of MLP under SLE and SE at 3 stages.

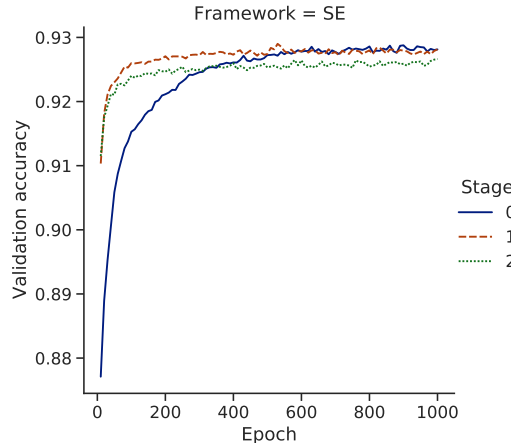


Figure 12: Converge statistics of SIGN under SE at 3 stages. SIGN+SLE is not reported due to OOM error.

Runtime experiments For runtime experiments on ogbn-products, the most of hyperparameters are kept the same. The batch sizes for training and inference are respectively set to 50000 and 100000 for all methods. The hidden dimensions of all methods are set to 512. The number of layers in MLP is 4. In both SIGN and SAGN, the number of layers in multi-hop MLP encoders is 2 and the number of post MLP encoder is 2. The number of aggregations in SIGN and SAGN is set to 5. 0-SLE means incorporating node label module. SIGN+0-SLE will encounter OOM error.

A.12 Visualization

The heatmap visualization of attention weights shows the global and local importances of different hops. We take SAGN on ogbn-products and ogbn-papers100M for examples. As shown in Figure 13, we can view the distribution of attention weights on ogbn-products. Neither adding node label module nor self-training affects the learned importances of hops. Compared to other hops, initial (0-hop) feature has obviously larger average weight. But it can be also small for some nodes. This implies that the raw node feature already contains important information and smoothed features can offer supplementary information. But the condition is very different on ogbn-papers100M, as shown in Figure 14. We can find that 2-hop and 3-hop are more important. With node label module, the importances become more homogeneous. SAGN+1-SE slightly changes the distribution compared

Table 10: Hyperparameter settings for ogbn-products including ablation studies.

Method	<i>lr</i>	<i>hidden</i>	<i>norm</i>	<i>L</i>	<i>K_f</i>	<i>K_l</i>	<i>drop</i>	<i>drop_a</i>	<i>drop_i</i>	<i>batch_size</i>	<i>a</i>	<i>wd</i>
MLP+SE	1e-3	512	row	4	9	-	0.5	-	0.2	50000	0.9	0
SIGN+SE	1e-3	512	row	2	5	-	0.4	-	0.3	50000	0.9	0
SAGN*+SE	1e-3	512	row	2	5	-	0.5	-	0.2	50000	0.9	0
SAGN**+SE	1e-3	512	row	2	5	-	0.5	-	0.2	50000	0.9	0
SAGN+SE	1e-3	512	row	2	5	-	0.5	0.4	0.2	50000	0.9	0
SLE	1e-3	512	row	4	-	9	0.5	-	-	50000	0.9	0
MLP+SLE	1e-3	512	row	4	9	9	0.5	-	0.2	50000	0.9	0
SIGN+SLE	1e-3	512	row	2	5	9	0.4	-	0.3	50000	0.9	0
SAGN*+SLE	1e-3	512	row	2	5	9	0.5	-	0.2	50000	0.9	0
SAGN**+SLE	1e-3	512	row	2	5	9	0.5	-	0.2	50000	0.9	0
SAGN+SLE	1e-3	512	row	2	3	9	0.5	0.4	0.2	50000	0.9	0

Table 11: Hyperparameter settings for ogbn-papers100M.

Method	<i>lr</i>	<i>hidden</i>	<i>norm</i>	<i>L</i>	<i>K_f</i>	<i>K_l</i>	<i>drop</i>	<i>drop_a</i>	<i>drop_i</i>	<i>batch_size</i>	<i>a</i>	<i>wd</i>
SAGN+SE	1e-3	1024	row	2	3	-	0.4	0.0	0.0	5000	0.7	0
SAGN+SLE	1e-3	1024	row	2	3	9	0.4	0.0	0.0	5000	0.7	0

with SAGN+0-SE. But it is restored for SAGN+2-SE. In addition, there exist obvious differences among nodes. This manifests as the different color blocks in the same column.

Table 12: Hyperparameter settings for ogbn-mag.

Method	<i>lr</i>	<i>hidden</i>	<i>norm</i>	<i>L</i>	<i>K_f</i>	<i>K_l</i>	<i>drop</i>	<i>drop_a</i>	<i>drop_i</i>	<i>batch_size</i>	<i>a</i>	<i>wd</i>
SAGN+SE	1e-3	1024	row	2	3	-	0.4	0.0	0.0	5000	0.7	0
SAGN+SLE	1e-3	1024	row	2	3	9	0.4	0.0	0.0	5000	0.7	0

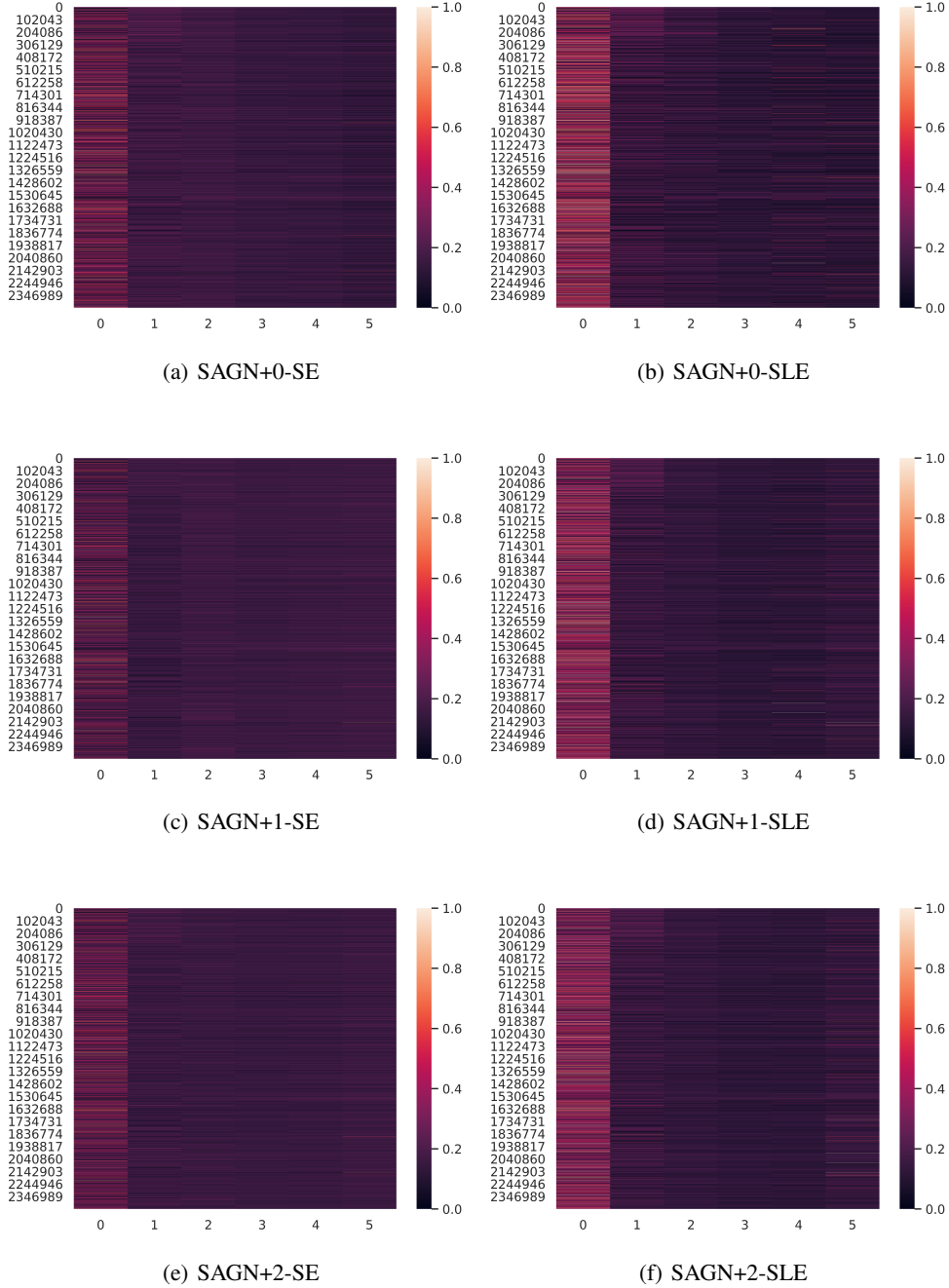


Figure 13: Heat map of attention weights. SAGN+SE and SAGN+SLE at different stages on ogbn-products are reported.

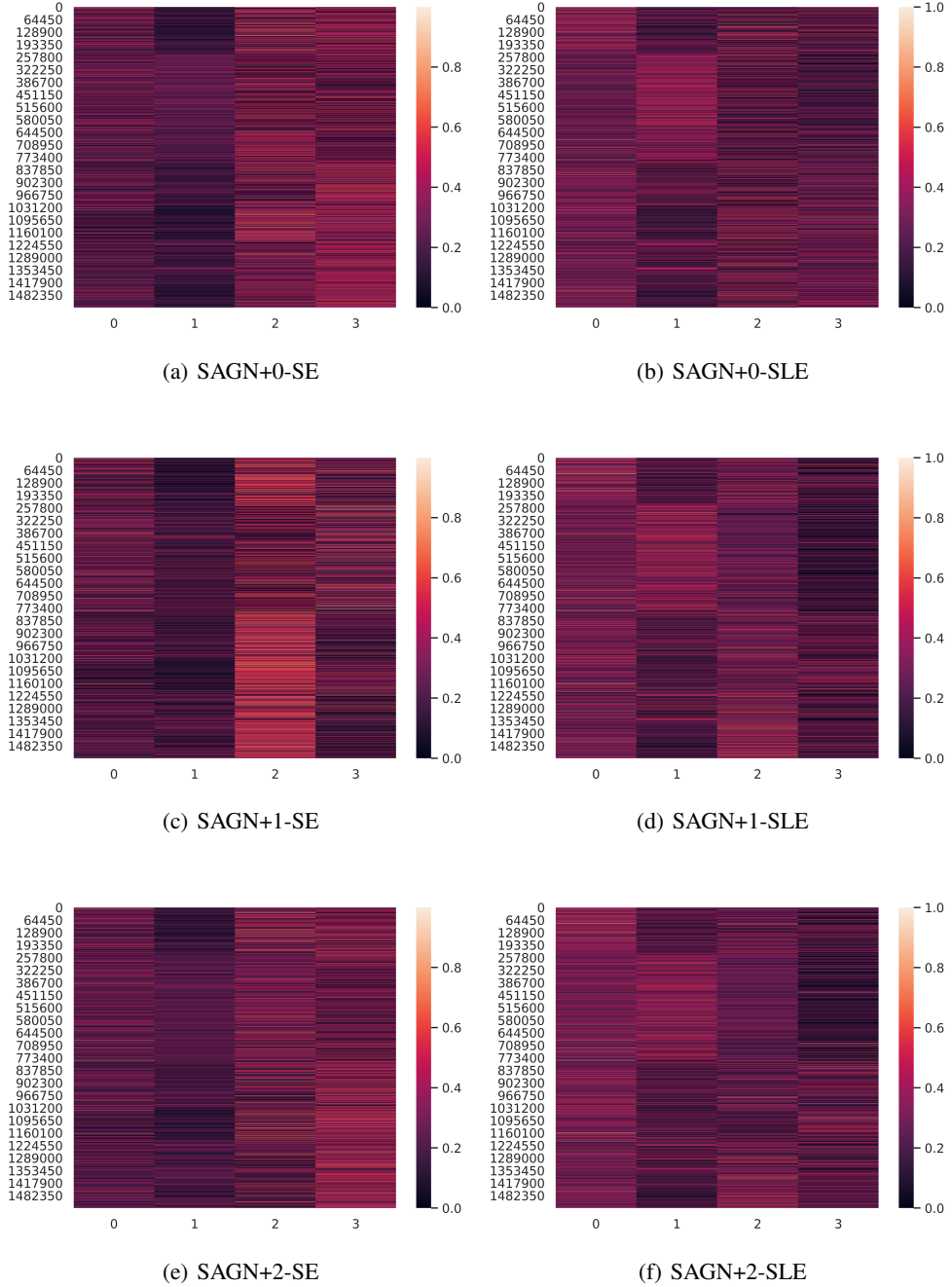


Figure 14: Heat map of attention weights. SAGN+SE and SAGN+SLE at different stages on ogbn-papers100M are reported.